Grid stabilization through VSC-HVDC using wide area measurements

Alexander Fuchs (*Member, IEEE*) , Sébastien Mariéthoz (*Member, IEEE*), Mats Larsson, and Manfred Morari (*Fellow, IEEE*)

***Abstract*—This work deals with the control of VSC-HVDC using wide area measurements. The goal is to enhance the transient and oscillatory stability of the power system for example during inter area oscillations or after faults. To this end, we present a predictive control framework that dynamically manipulates both the active and reactive powers injected by the VSC-HVDC links in a grid of generators, lines and loads. The approach naturally adresses two difficulties of the control problem: First, power injections by the VSC-HVDC are limited by constraints that depend on the state of the power system. Second, wide area measurements communicated to the controller are subject to a time varying delay. The simulations show a benchmark example of four generators linked by a VSC-HVDC. With the proposed approach, the VSC-HVDC can control this example system to an instable operating point while respecting the system constraints and compensating measurement delays.**

***Index Terms*—VSC-HVDC, MPC, transient stability, oscillatory stability, wide area measurements**

I. Introduction

Power transmission systems have to react flexibly to gradual load flow changes to ensure *small signal stability* of the generator angles. They also have to overcome the impact of large disturbances, such as faults, to ensure *transient stability* [1]. Both stability issues become increasingly challenging as the transmission systems are operated with more power flow fluctuations due to energy trade and renewable energy sources. VSC-HVDC transmission links allow the independent control of active and reactive power injected at the converter stations, thereby providing an increased controllability of the power system compared to conventional lines or classical CSC-HVDC. Optimizing the power injections of the VSC-HVDC on a slow time scale can be used to improve damping behaviour, capacity margins and voltage stability [2], [3]. Optimizing the steady state loadability through changes of the setpoint in contingency cases has been studied in [4]. Here we extend to a dynamic framework to tackle also oscillatory and transient stability. A potential for power system enhancement lies in *adjusting the power injections* of the VSC-HVDC during transients of the system using the information from Wide Area Measurement Systems (WAMS), as suggested in [5]. Some control schemes that are using WAMS in combination with FACTS devices to enhance power system stability are discussed in [6]. This paper adresses the same problem with a focus on the control part, in particular when using VSC-HVDC transmission.

The injections of the VSC-HVDC have to be chosen carefully to avoid a negative impact on the power system stability. This issue has been adressed using Control Lyapunov Functions in [7] where a global energy function is constructed and also in [8] with coordinated fuzzy control of VSC-HVDC and classical Power System Stabilizers. Both approaches do not explicitly incorporate constraints. During critical transients the system is likely to reach its limits which should be taken into account by the controller to maintain the system in a safe mode.

Another issue originates from delays in the system, mainly caused by the communication channels for measurement and control signals. In this work, the estimator will be represented by a delay-perturbation model. The investigation of the estimation strategy itself is out of the scope of this paper, see for instance Chapter 11 in [6] for an introduction on WAMS.

The goal of the paper is to derive a control framework for power grid stabilization through VSC-HVDC links. The controller ensures the transient and mid-term stability of the generator angles while respecting the system constraints. We propose a predictive control scheme based on [9] where the effectiveness of the approach was illustrated on a small power system example without measurement delay. The small size of the power system in [9] allowed to use the closed form solution of the power flow equations to derive a prediction model for the controller. We extend the control framework to multi machine power systems with multiple VSC-HVDC by avoiding the analytic solution of the power flow equations.

The hierarchical control scheme has two loops. The outer loop ensures power system stability by setting the references for the power injections of the VSC-HVDC. The inner loops ensure fast and accurate tracking of these references using high dynamic performance controllers. In this paper we focus on the design of the outer control loop. For details of the inner control loops used in our studies, see [9], [10].

The paper is organised as follows. Section II presents the control problem and provides the models for the power system with measurement units and VSC-HVDC. Section III derives the predictive control scheme that manipulates the injections of the VSC-HVDC to drive the power system to a given reference state while respecting the system constraints. Section IV applies the control scheme to a benchmark power system with two areas, using only VSC-HVDC for stabilization.

A. Fuchs , S. Mariéthoz and M. Morari are with the Automatic Control Laboratory, Swiss Federal Institute of Technology (ETH Zürich), Physikstrasse 3, CH - 8092, Zürich, Switzerland. E-mail: fuchs@control.ee.ethz.ch

M. Larsson is with ABB corporate research, Baden, Switzerland.

The authors thank their funding partners swisselectric research and ABB corporate research, Switzerland.

978-1-4244-8417-1/11/$26.00 ©2011

II. Power system model

This section defines the model of the power system, the measurement units and the system constraints. The model will be used in the next sections to derive the model predictive control scheme and for the simulations.

A. Basic network equations

Consider a power grid with generators, VSC-HVDC links and constant impedance loads. Given a grid of n_g generators, n_h buses connected to an HVDC converter and n_l buses connected to loads, denote the vector of complex voltages at these buses by V_g, V_h and V_l. Similarly, define the vectors I_g and I_h of complex currents injected at the generator and voltage buses. The phasors $I_{g,i}$ and $V_{g,i}$ represent the current injection and the voltage at the i'th generator bus. This allows to write the $n_g + n_h + n_l$ Kirchhoff equations

$$\begin{pmatrix} I_g \\ I_h \\ 0 \end{pmatrix} = \begin{pmatrix} Y_1 & Y_2 & Y_3 \\ Y_2^T & Y_4 & Y_5 \\ Y_3^T & Y_5^T & Y_6 \end{pmatrix} \begin{pmatrix} V_g \\ V_h \\ V_l \end{pmatrix} \quad , \tag{1}$$

which can be reduced to n_g equations

$$I_g = M_{g1} V_g + M_{g2} I_h \tag{2}$$

using the complex matrices

$$M_{g1} = Y_1 - (Y_2 \; Y_3) \begin{pmatrix} Y_4 & Y_5 \\ Y_5^T & Y_6 \end{pmatrix}^{-1} \begin{pmatrix} Y_2^T \\ Y_3^T \end{pmatrix} \quad , \tag{3}$$

$$M_{g2} = (Y_2 \; Y_3) \begin{pmatrix} Y_4 & Y_5 \\ Y_5^T & Y_6 \end{pmatrix}^{-1} \begin{pmatrix} I \\ 0 \end{pmatrix} \quad . \tag{4}$$

The reduction can be always done when the power network forms a connected graph [11]. The second order model of the i'th generator angle θ_i is given by the swing equation

$$2H_i \ddot{\theta}_i = P_{m,i} - P_{e,i} - D_i \dot{\theta}_i \quad , \tag{5}$$

with the electromechanical power

$$P_{e_i} = \Re(V_{g,i} I_{g,i}^*) \quad , \tag{6}$$

$$V_{g,i} = |V_{g,i}| e^{j \cdot \theta_i} \quad . \tag{7}$$

If the parameters H_i, D_i, the mechanical generator powers $P_{m,i}$, the excitation voltages $|V_{g,i}|$ $(i = 1, ..., n_g)$ and the current injections $I_{h,m} = I_{h,m}^{re} + j \cdot I_{h,m}^{im} (m = 1, 2, ..., n_h)$ are given, then (2)-(7) is a system of ordinary differential equations (ODEs) representing the dynamics of the power system.

The paper studies the effect of the VSC-HVDC injections neglecting other stabilizing controllers that manipulate the generator's $P_{m,i}$ or $|V_{g,i}|$. Therefore, from the controller perspective, the generator equation (5) is a system with $2 \cdot n_g$ dynamic states (generator angles θ_i and angular speed $\dot{\theta}_i$) and $2 \cdot n_h$ control inputs (HVDC current injections $I_{g,i}^{re}$ and $I_{g,i}^{im}$).

In the basic network model, the VSC-HVDC is modeled as an ideal current source, that instantaneously injects the AC-current chosen by the controller. The model can be extended for a more detailed description of the generators or the HVDC link dynamics. The control framework described in Section III does not change as long as the power system model is described by a set of ODEs.

B. Wide area measurements and communication

Estimating the voltage phase angle based on time domain measurements is a well studied problem, see [12] and reference therein. A Wide Area Measurement System (WAMS) combines the estimates of multiple phase measurement units from different points of the power system [6], [12]. Reference [13] demonstrates how to estimate the generator angles based on the PMU data We model the estimated generator angle $\hat{\theta}_i$ as perturbed and delayed estimate of the actual angle θ_i:

$$\hat{\theta}_i(t_k) = \theta_i(t_k - \tau_k) + d_i \quad . \tag{8}$$

The estimates are available at discrete times t_k where the time intervals $t_k - t_{k-1}$ are not required to be constant in size, accounting for informations losses on the communication channel. The time delay τ_k of the estimate is assumed to be known. A similar model represents the delay of the generator angular speed $\hat{\dot{\theta}}_i$ and the delay due to the computation and communication of the control signal.

C. Power system constraints

Constraints of the power system presented in Section II-A occur as linear and nonlinear equalities and inequalities on the dynamic states and the VSC-HVDC injections.

A typical constraint for AC-DC converters is the active power equality [14], written for the i'th HVDC bus :

$$P_{AC} = \Re(V_{h,i} I_{h,i}^*) = U_{DC} \cdot I_{DC} = P_{DC} \quad . \tag{9}$$

The AC current injected by the VSC-HVDC is limited in magnitude,

$$|I_{h,i}| \leq I_{AC,max} \quad , \tag{10}$$

and the DC voltage yields an upper bound on the magnitude of the AC voltage at the converter terminals,

$$|V_{h,i} + Z \cdot I_{h,i}| \leq U_{DC} \quad , \tag{11}$$

where the complex impedance Z represents the converter station series reactance including the filters. Finally, the DC-current of the VSC-HVDC is constrained,

$$|I_{DC}| \leq I_{DC,max} \quad . \tag{12}$$

Constraints (9)-(12) have to be respected by any controller that manipulates the VSC-HVDC during transients of the power system. Further constraints can be added, for instance to bound the AC voltage level at other buses of the grid or to limit the rate of change of the generator angles and the DC current.

III. Predictive power system control

This section describes the predictive control scheme that stabilizes the generator angles by manipulating the AC-currents injected by the VSC-HVDC.

First, the power system model is approximated by linear discrete time prediction model. Second, the nonlinear constraints are approximated by linear constraints. After these preliminary steps, we can formulate an optimization problem that can be efficiently solved in real time to determine the injections of the VSC-HVDC online.

A. Linearized discrete network equations

The power system model (2)-(7) corresponds to a set of ordinary differential equations

$$\dot{x} = f(x, u) \tag{13}$$

with the dynamic states x and the inputs u:

$$x = (\theta_1, ..., \theta_{n_g}, \dot{\theta}_1, ..., \dot{\theta}_{n_g})^T \in \mathbb{R}^{2 \cdot n_g} \tag{14}$$

$$u = (I^{re}_{h,1}, ..., I^{re}_{h,n_h}, I^{im}_{h,1}, ..., I^{im}_{h,n_h})^T \in \mathbb{R}^{2 \cdot n_h} \tag{15}$$

A steady state operating point (x_{ss}, u_{ss}) has to satisfy the set of nonlinear algebraic equations

$$0 = f(x_{ss}, u_{ss}) \quad , \tag{16}$$

and is assumed to be provided. Linearization about this operating point yields the matrices

$$\hat{A} = \frac{\partial f}{\partial x}(x_{ss}, u_{ss}) \quad \hat{B} = \frac{\partial f}{\partial u}(x_{ss}, u_{ss}) \tag{17}$$

which define the continuous time dynamics

$$\dot{\tilde{x}} = \hat{A}\tilde{x} + \hat{B}\tilde{u} \tag{18}$$

of the steady state deviations

$$\tilde{x}(t) = x(t) - x_{ss} \qquad \tilde{u}(t) = u(t) - u_{ss} \tag{19}$$

For a given time step T, (18) can be discretized using Euler forward discretization :

$$\begin{aligned} \tilde{x}_{k+1} &= \tilde{x}((k+1)T) = A\tilde{x}(kT) + B\tilde{u}(kT) \\ &= A\tilde{x}_k + B\tilde{u}_k \end{aligned} \tag{20}$$

with

$$A = I + \hat{A}T \qquad B = \hat{B}T \quad . \tag{21}$$

The time step T corresponds to the length of the sampling interval of the controller, during which the control signal u is kept constant.

B. Compensating system delays

As discussed in Section II-B the power system model includes time varying delays on the measurements and the control signals. Delays can be easily included in the predictive control framework by augmenting the state space of the linear prediction model to store the past control inputs applied during the delay interval (see Chapter 2.5 in [15]).

The simulation example in Section IV illustrates that the control scheme has a certain robustness even when simply ignoring the delays.

C. Respecting the system constraints

The power system constraints presented in Section II-C can be expressed in terms of the x and u:

$$g_1(x, u) = 0 \qquad g_2(x, u) \leq 0 \tag{22}$$

The set of permissible states and injections satisfying (22) is a nonconvex subset of $\mathbb{R}^{2(n_g + n_h)}$. The (linear) predictive control formulation requires a convex approximation of the constraint set, written in the form

$$H_1\tilde{x}_k + H_2\tilde{u}_k \leq H_3 \tag{23}$$

$$H_4\tilde{x}_k + H_5\tilde{u}_k = H_6 \tag{24}$$

From (1), it is possible to derive, similar to (2),

$$V_h = M_{h1}V_g + M_{h2}I_h \quad , \tag{25}$$

for some complex matrices M_{h1} and M_{h2}.

This allows to rewrite the constraints (10) and (11) in a form that depends linearly on V_g and the manipulated variables $(I^{re}_{h,i}, I^{im}_{h,i})$. As seen in (7), $V_{g,i}$ is a function of the dynamic state θ_i and can therefore not change abruptly. Using the linearization of $V_{g,i}$ in (7) for small deviations of the angle θ_i from its current value yields the constraints (10) and (11) in the desired form (23).

Constraint (12) is, due to (9) and for a given nonzero DC voltage U_{DC}, equivalent to

$$|\Re(V_{h,i}I^*_{h,i})| \leq \frac{I_{DC,max}}{U_{DC}} \quad . \tag{26}$$

Substituting (25), it is apparent that (26) is a quadratic inequality constraint on the manipulated variables (I^{re}_h, I^{im}_h). The constraint can not be included directly in the problem formulation since, on the time scales of electromechanical stability effects, I_h, the AC current injected by the VSC-HVDC, may significantly change and a linearization would be overly restrictive. Another possibility is to simply relax the problem by ignoring the constraint (12) for the computation of the control law. In practise, the low level VSC-HVDC controller will ensure that the constraint is satisfied. In this paper, we model this effect by a simple saturation of the control input.

D. Predictive control

This section presents the model predictive control (MPC) scheme that stabilizes the grid by manipulating the reference values for the VSC-HVDC power. An optimization problem is solved to determine the control input of the next N time steps [15]. The optimization problem solved is a quadratic program (QP) with weight matrices $\bar{P}$, $\bar{Q}$ and $\bar{R}$ that can be solved efficiently in real-time [10].

$$\begin{aligned} \min_{\tilde{u}_k, ..., \tilde{u}_{k+N-1}} \quad & \sum_{l=k}^{k+N-1} (\tilde{x}_l^T \bar{Q} \tilde{x}_l + \tilde{u}_l^T \bar{R} \tilde{u}_l) + \tilde{x}_{k+N}^T \bar{P} \tilde{x}_{k+N} \\ \text{s.t.} \quad & \forall l \in \{k, 1, ..., k+N-1\} \\ & \tilde{x}_{l+1} = A(\tilde{x}_l - x_{ss}) + B(\tilde{u}_l - u_{ss}) \\ & H_1\tilde{x}_l + H_2\tilde{u}_l \leq H_3 \\ & H_4\tilde{x}_l + H_5\tilde{u}_l = H_6 \end{aligned} \tag{27}$$

The initial value $\tilde{x}_k$ is determined from the measurements. After the optimization problem has been solved, the first element of the optimal solution, $\tilde{u}_0$, is used to compute the reference of the VSC-HVDC,

$$u = u_{ss} + \tilde{u}_0 = (I^{re}_{h,1}, ..., I^{im}_{h,n_h})^T \quad . \tag{28}$$

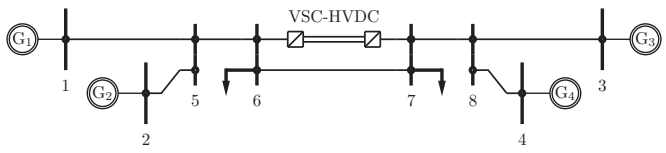

Fig. 1. Example power system for simulation: AC links (lines) and loads (arrows) modeled as complex impedances, generators (G_i) modeled as second order model, VSC-HVDC link modeled as injection model

The time is then incremented and the procedure repeated. This concept is know as *receding horizon control* or model predictive control (MPC).

A typical choice for the cost function weights are diagonal matrices $\bar{Q} = I$ and $\bar{R} = r \cdot I$.

The cost function captures the minimization of the generators angular error, its time derivative and the deviation of the injected currents from their steady state values. The scaling parameter r represents the tradeoff between minimizing the control effort and minimizing the state deviation. The terminal weight $\bar{P}$ is chosen as the terminal weight of the infinite horizon LQR controller of system (20).

For all simulation examples in this paper we will use $\bar{R} = r \cdot I$ with $r = 0.1$ and $\bar{Q} = \mathrm{diag}(0\ I)$, which penalizes only the angular frequency deviation of the generators from the common setpoint.

IV. Simulation study: concept verification

A. Simulation Example

To verify the performance of the controller, a power grid consisting of four generators in two areas, coupled by a weak AC line, is considered. The system has been often used as test system in the literature and a detailed description with all necessary parameters is given in Example 12.6 of [1]. As modification, an VSC-HVDC link is placed in parallel to the weak AC link as illustrated in Fig. 1. The original example system was used to illustrate the effectiveness of Power System Stabilizer and other control actions acting on the generators, to damp inter area oscillations and ensure transient stability. In this study, all such control actions are neglected to study the effect of the VSC-HVDC with the proposed control scheme independently.

The objective is to control the system to the steady state

$$x_{ss} = (\theta_{ss}^T,\ \dot{\theta}_{ss}^T)^T \tag{29}$$

$$\theta_{ss} = (0, -0.0168, -0.2998, -0.3235)^T \tag{30}$$

$$\dot{\theta}_{ss} = (0, 0, 0, 0)^T \quad , \tag{31}$$

with the steady state injections

$$u_{ss} = (I_{h,1,ss},\ I_{h,2,ss})^T \tag{32}$$

$$I_{h,1,ss} = 2.4017 - j \cdot 0.2561 \tag{33}$$

$$I_{h,2,ss} = -1.7471 + j \cdot 1.5707 \quad . \tag{34}$$

In a practical case we would have a preprocessing step where we compute the desired generator angles θ_{ss} from the power reference of the generators. Assuming the desired power flow distribution is known, it can be inserted in (16) whos solution will provide the numerical values of (29)-(34). Note that this steady state does not correspond to an actual optimal power flow solution, but is only intended to illustrate the stabilizing effects of the proposed control scheme. In particular, the Jacobi matrix $\hat{A}$ as in (17) has one of the eight eigenvalues with positive real part, 2.4661, making the equilibrium point (x_{ss}, u_{ss}) unstable.

For all simulations, the initial state of the first generator angle is perturbed by 0.1 rad, all other states start at their steady state value. The predictive controller has to stabilize the system, while respecting the power system contraints. All constraints on the AC current injected by the HVDC are absorbed in a simple bound the real and imaginary part of the complex current:

$$|I_{h,i}^{re}| \leq 2.9 \qquad |I_{h,i}^{im}| \leq 2.9 \qquad i = 1, 2 \tag{35}$$

We also require the deviations of the generator angles to be bounded,

$$|\theta_i - \theta_{ss,i}| \leq \delta_{max} \tag{36}$$

for different $\delta_{max} \in \{1 \text{ rad}, 0.2 \text{ rad}, 0.1 \text{ rad}\}$.

The controller time step is 20 ms, which also equals the interval of the grid measurements. Additionally, the measurements are modeled as in (8), without the disturbance ($d_i = 0$) but with a delay τ_k, ranging from 0 to 100 ms.

Several simulations are carried out over 10 seconds each, using the the initial perturbation of the first generator angle and different constraints and delay values.

B. Comparison to constant HVDC references

We first study the problem without delays. Fig. 2 shows the trajectories of the generator angles without the proposed control scheme, where the injections of the VSC-HVDC are kept constant. The generators angles (bold lines) accelerate away from the equilibrium (dashed lines) to a different steady state that corresponds to different powers provided to the loads of the system.

In contrast, Fig. 3 shows the generator angles trajectories (bold lines) when using the predictive control scheme with $\delta_{max} = 1$ rad. It can be seen that after initial transients, the angles (bold lines) are recovered and converge to the unstable equilibrium (dashed lines).

C. Respecting the constraints

For the simulation, with $\delta_{max} = 1$ rad, Fig. 4 shows how the controller respects the prescribed bounds on the current injections.

Equivalently, Fig. 5 shows the angular deviation of generator 1 from the steady state $\theta_{ss,1} = 0$ using three different angular constraints δ_{max}. The controller exploits the prescribed bounds as much as possible. As expected, the transient of the active power transmitted over the HVDC link becomes rougher as the constraints are tightened, see Fig. 6.

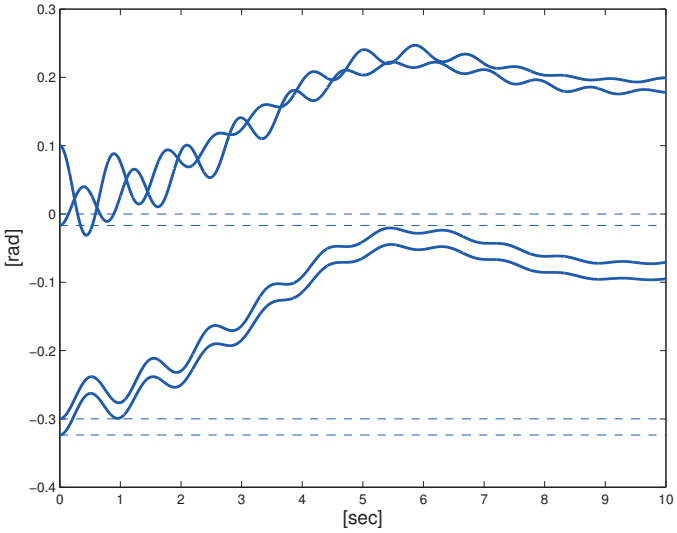

Fig. 2. Generator angles: With constant HVDC injections, the angles (bold) move away from the equilibrium (dashed)

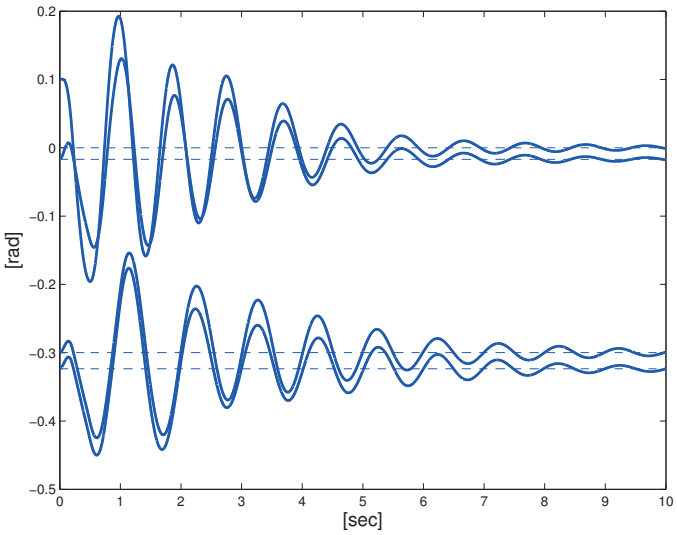

Fig. 3. Generator angles: The HVDC power injections are adjusted using the proposed control scheme to keep the angles (bold) within limits and bring them to an equilibrium (dashed). Compare to Fig. 1 with constant HVDC power injections.

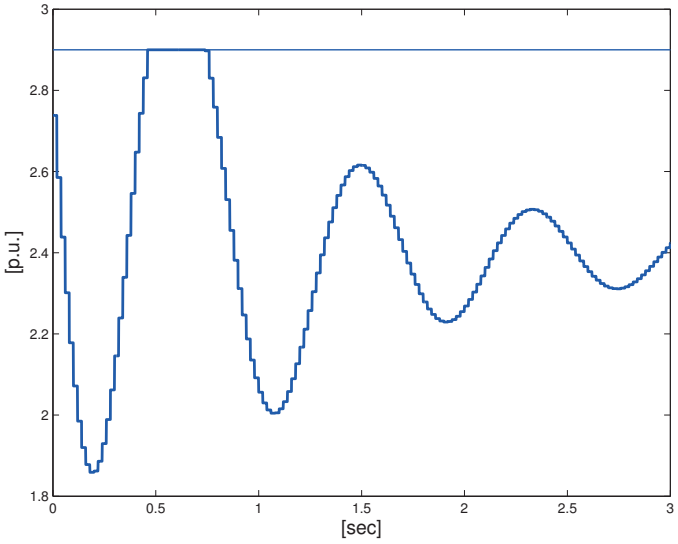

Fig. 4. Real component of the AC-current injected by the left inverter: During transient, HVDC AC-current reference (bold) is kept within limits (2.9 p.u., horizontal line).

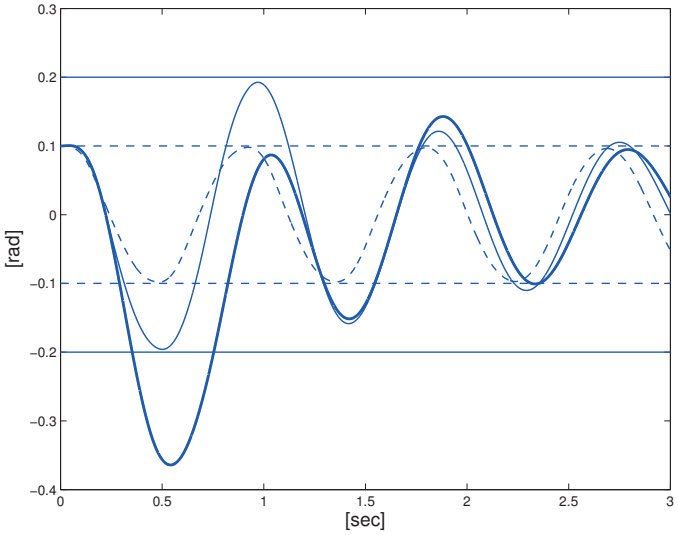

Fig. 5. Angle of generator 1 for different controller constraints: During transient, generator angle deviation respects prescribed tolerances (horizontal lines) of $\delta_{max} = 1$ rad (bold), 0.2 rad (thin solid) and 0.1 rad (dashed)

D. Robustness to measurement delay

Finally, we compare in Fig. 7 the angular deviation of the first generator for $\delta_{max} = 1$ rad and different (constant) values of the measurement delay up to 100 ms. The amplitudes of the first swings increase as τ_k becomes longer, but the oscillations are damped out.

V. Conclusion

A framework for the transient stabilization of power grids using VSC-HVDC and MPC has been presented. For control purposes, the power system equations were converted to a linear discrete time system. Equality and inequality constraints on the states of the power grid and the VSC-HVDC are naturally included in the problem formulation. The effectiveness of the approach is illustrated with a multi-generator example with the HVDC modeled as an ideal current source. The system is controlled to an unstable equilibrium under measurement delay and with no additional means of grid control, besides the VSC-HVDC. Further studies should investigate the measurement uncertainty and the handling of constraints that are nonlinear in the control inputs.

References

[1] P. Kundur. *Power System Stability and Control*. McGraw-Hill, Inc., 1993.

[2] S. Johansson. Power sytems stability with VSC DC-transmission systems. In *Cigré Conference in Paris, France*, 2004.

[3] C. Rehtanz and K. Sengbusch. Lastflusssteuerung zur systemstabilisierung. In *ETG/BDEW-Tutorial Schutz- und Leittechnik*, Fulda, Germany, November 2008.

[4] G. Hug-Glanzmann. *Coordinated Power Flow Control to Enhance Steady-State Security in Power Systems* . PhD thesis, ETH Zurich, Switzerland, May 2008.

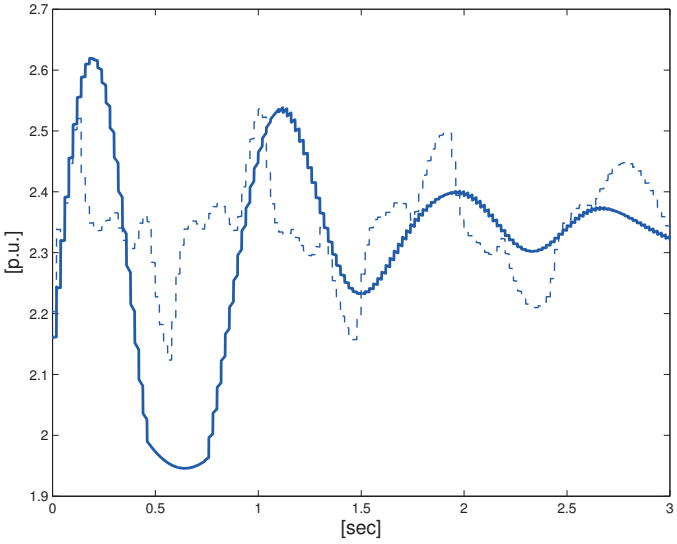

Fig. 6. Active power through HVDC line for two different controller constraints: A larger tolerance of the generator angle ($\delta_{max} = 1$ rad) allows a smoother transient of the active power transmitted (bold). Compare to the active power transient (dashed) for a small tolerance of the generator angle ($\delta_{max} = 0.1$ rad).

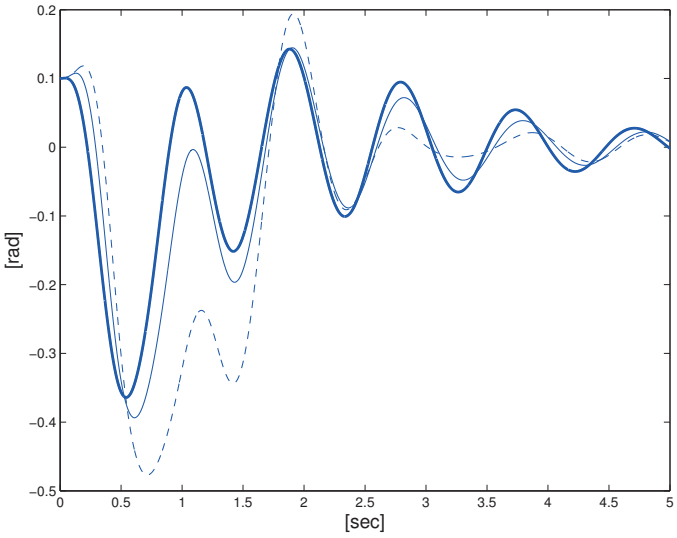

Fig. 7. Angle of generator 1 for different measurement delays: No delay (bold), 20 ms (thin solid), 100 ms (dashed). With increasing delay, performance degrades gracefully.

[5] J. Pan, R. Nuqui, K. Srivastava, T. Jonsson, P. Holmberg, and Y. Hafner. Ac grid with embedded vsc-hvdc for secure and efficient power delivery. In *IEEE Energy 2030*, Atlanta, USA, November 2008.

[6] B. Pal X. Zhang, C. Rehtanz. *Flexible AC transmission systems: modelling and control*. Springer-Verlag, 2006.

[7] H.F. Latorre, M. Ghandhari, and L. Soder. Multichoice control strategy for VSC-HVdc. In *Bulk Power System Dynamics and Control - VII. Revitalizing Operational Reliability, 2007 iREP Symposium*, 2007.

[8] R.Y. Chen, Y. Zhang, L. Quo, and M. Wei. Online coordinated control of adaptive-network-based fuzzy power system stabilizers and HVDC modulation controller. In *Power Engineering Conference, 2007. IPEC 2007. International*, pages 889–892, March 2007.

[9] A.N. Fuchs, S. Mariéthoz, M. Larsson, and M. Morari. Constrained optimal control of VSC-HVDC for power system enhancement. In *IEEE Powercon, Power System Technology*, Hangzhou, China, October 2010.

[10] S. Richter, C.N. Jones, and M. Morari. Real-Time Input-Constrained MPC Using Fast Gradient Methods. In *Conference on Decision and Control, CDC*, Shanghai, China, December 2009.

[11] F. Doerfler and F. Bullo. Synchronization of power networks: Network reduction and effective resistance. In *IFAC Workshop on Distributed Estimation and Control in Networked Systems*, pages 197–202, Annecy, France, September 2010.

[12] A.G. Phadke and J.S. Thorp. *Synchronized Phasor Measurements and Their Applications*. Springer, 2008.

[13] A. Del Angel, P.Geurts, D. Ernst, G. Mevludin, and L. Wehenkel. Estimation of rotor angles of synchronous machines using artificial neural networks and local pmu-based quantities. *Neurocomputing*, 70:2668–2678, 2007.

[14] D.Jovcic, L.A.Lamont, and L.Xu. VSC transmission model for analytical studies. In *IEEE PES General Meeting*, pages 1737–1742, 2003.

[15] J. Maciejowski. *Predictive Control with Constraints*. Prentice Hall, 2001.

Alexander Fuchs (S'10) pursues his doctorate at the Automatic Control Laboratory at ETH Zurich. Before, he studied at the Technical University of Dresden (Germany), Ecole Centrale Paris (France) and the University of Texas at Austin (USA), graduating in mechatronics and aerospace engineering. His diploma thesis focused on parameter clustering for robust pose estimation. He is interested in model predictive control with applications to power systems, in particular HVDC transmission.

Sébastien Mariéthoz (M'05) received the Ph.D. degree in electrical engineering for his work on asymmetrical multilevel converters from EPFL, Lausanne, Switzerland in 2005. He was research fellow with the PEMC group, University of Nottingham, UK, focusing on the design and control of new matrix converter topologies. He joined the Automatic Control Laboratory, ETH Zürich in 2006, where he is currently senior researcher. His current research interests include power converter topologies, control of power electronic systems with emphasis on model predictive control and sensorless control techniques.

Mats Larsson received his Master's degree (Computer Science and Engineering), Licentiate (Industrial Automation), and PhD (Industrial Automation) Degrees from Lund University, Sweden in 1993, 1997 and 2001, respectively. Since 2001 he has been employed by Corporate Research, ABB Switzerland. He is a Principal scientist responsible for the research and development of phasor measurement applications and wide-area stability controls for power systems. His research interests include HVDC, power system stability and applications of optimal control and system identification in power systems.

Manfred Morari (F'05) was appointed head of the Automatic Control Laboratory at ETH Zurich in 1994. Before that he was the McCollum-Corcoran Professor of Chemical Engineering and Executive Officer for Control and Dynamical Systems at the California Institute of Technology. He obtained the diploma from ETH Zurich and the Ph.D. from the University of Minnesota, both in chemical engineering. His interests are in hybrid systems and the control of biomedical systems.